Supporting Information for

Alternative dynamic regimes of plankton communities in extreme environments

Guido Occhipinti, Davide Valenti and Paolo Lazzari

Guido Occhipinti
E-mail: gocchipinti@ogs.it

This PDF file includes:

Supporting Information Text

Additional Figures. Here, we show additional figures which can help the discussion of the results presented in the main text. Figures S1-S8 show all the solutions of the experiment EXP-SEQ, described in Sections 2.3.1 and 3.1 (main text). The response to oxygen nudging and decrease in air temperature has been omitted because it did not add interesting results, as explained in the main text. The solutions of EXP-INI, described in Sections 2.3.2 and 3.2 (main text), under the phosphate nudging forcing are shown in Fig.S9.

Biogeochemical Flux Model (BFM) equations. Here we present a selection of the equations of the BFM, which can give a general overview of the complexity of the model (see also a representation of the modeled processes in Fig.S10a). The biogeochemical component of the BFM is formulated as a system of $N_{tot} = 54$ ordinary nonlinear differential equations and represented by a N_{tot}-dimensional state vector $\mathbf{x}$. The time derivatives of a generic phytoplankton carbon component (e.g., carbon in diatom, $x^i = P1_c$) and of the corresponding nutrient component (e.g. nitrogen in diatom, $x^j = P1_n$) are given by:

$$\frac{\partial x^i}{\partial t} = f_c^{gpp}(\mathbf{x}) - f_c^{rsp}(\mathbf{x}) - f_c^{exc}(\mathbf{x}) - f_c^{prd}(\mathbf{x}), \tag{1}$$

$$\frac{\partial x^j}{\partial t} = f_n^{upt}(\mathbf{x}) - f_n^{rel}(\mathbf{x}) - f_n^{prd}(\mathbf{x}). \tag{2}$$

The f-s are continuous functions representing the biogeochemical fluxes associated with the main physiological processes. *gpp* is the gross primary production (expressed in $mgC\ m^{-3}\ day^{-1}$) and represents photosynthesis (i.e. the flux of inorganic CO_2 to organic compounds). Respiration (*rsp*) refers to the release of carbon (production of CO_2). Excretion processes (*exc*) are related to the metabolic activities of cells and the need to balance the internal carbon quota with other elements. In fact, in case of phosphate and nitrate shortage *gpp* might produce a too high carbon to phosphorus (or carbon to nitrogen) ratio in the organism, and in this case an appropriate amount of organic carbon must be released into the environment as dissolved organic carbon (DOC). *prd* is predation or grazing by zooplankton. The f-s are factorised in a number of regulating functions, e.g.

$$f_{gpp}(\mathbf{x}) = r_{max}f_T(T)f_I(I)f_{nut}(\mathbf{x})x^i, \tag{3}$$

where r_{max} is the (specie specific) maximum growth rate, $f_I(I)$ is an irradiance (I) harvest factor, and $f_T(T)$ is the dependence of metabolic rates on temperature (T). f_{nut} define the limitation to growth caused by nutrient depleted conditions. The temperature regulation factor $f_T(T)$ is given, for example, by the following expression (1):

$$f_T(T) = Q^{\frac{T-T_{ref}}{T_{ref}}} - Q^{\frac{T-T_{thresh}}{3°C}} \tag{4}$$

where the dimensionless parameter Q is 2.00 for all organisms except the heterotrophic bacteria (B1), whose Q is 2.95 (1–4). The reference temperature (T_{ref}) is set at $10°C$ and the threshold temperature (T_{thresh}) is set at $32°C$. The same temperature regulating factor ($f_T(T)$) acts on the other physiological processes. Consequently, higher temperatures increase the overall metabolic rates and accelerate the biogeochemical cycling of the system up to a threshold (T_{thresh}), after which the rates slowly decreases (see Fig.S11, representing enzyme degradation at high temperatures (5).

The equations for zooplankton are similar to those for phytoplankton. In this case, the photosynthetic growth term is replaced by the grazing term (f_{gra}). As an example, in the case of carnivorous mesozooplankton carbon component ($x^i = Z3_c$) we obtain

$$\frac{\partial x^i}{\partial t} = f_{gra}(\mathbf{x}) - f_{rsp}(\mathbf{x}) - f_{rel}(\mathbf{x}) - f_{prd}(\mathbf{x}). \tag{5}$$

The total amount of food available to zooplankton is calculated by adding the possible prey items (see Fig. S10b) weighted by the predator's food preferences. Grazing analytic form follows a type 2 form (6):

$$f_{gra}(\mathbf{x}) = f_T(T)r_{max}\frac{F_c}{F_c + h_z}x^i, \tag{6}$$

$$F_c = \sum_{j \in preyC} \delta^j e^j x^j, \tag{7}$$

$$e^j = \frac{x^j}{x^j + \mu_Z}, \tag{8}$$

where h_z is a parameter inversely related to the mobility and searching volume of the organism, x^j is the carbon content in the prey, and δ^j is the preference for a specific prey.

The cycles of dissolved inorganic nutrients are essential components of ocean biogeochemical models. In the BFM five inorganic compounds are considered: phosphate, nitrate (nitrate + nitrite), ammonium, silicate and iron. The nutrient cycles are described by ordinary differential equations, similar to those used for plankton. As an example, the cycle of phosphate $x^i = N^{(1)}$ is modelled as follows

$$\frac{dx^i}{dt} = -\sum_{j \in phytoP} \frac{dx^j}{dt}\bigg|_{x^i}^{upt} + \sum_{j \in bacP} f_j^p \frac{dx^j}{dt}\bigg|_{x^i}^{upt,rel} + \sum_{j \in zooP} \frac{dx^j}{dt}\bigg|_{x^i}^{rel}. \tag{9}$$

Guido Occhipinti, Davide Valenti and Paolo Lazzari
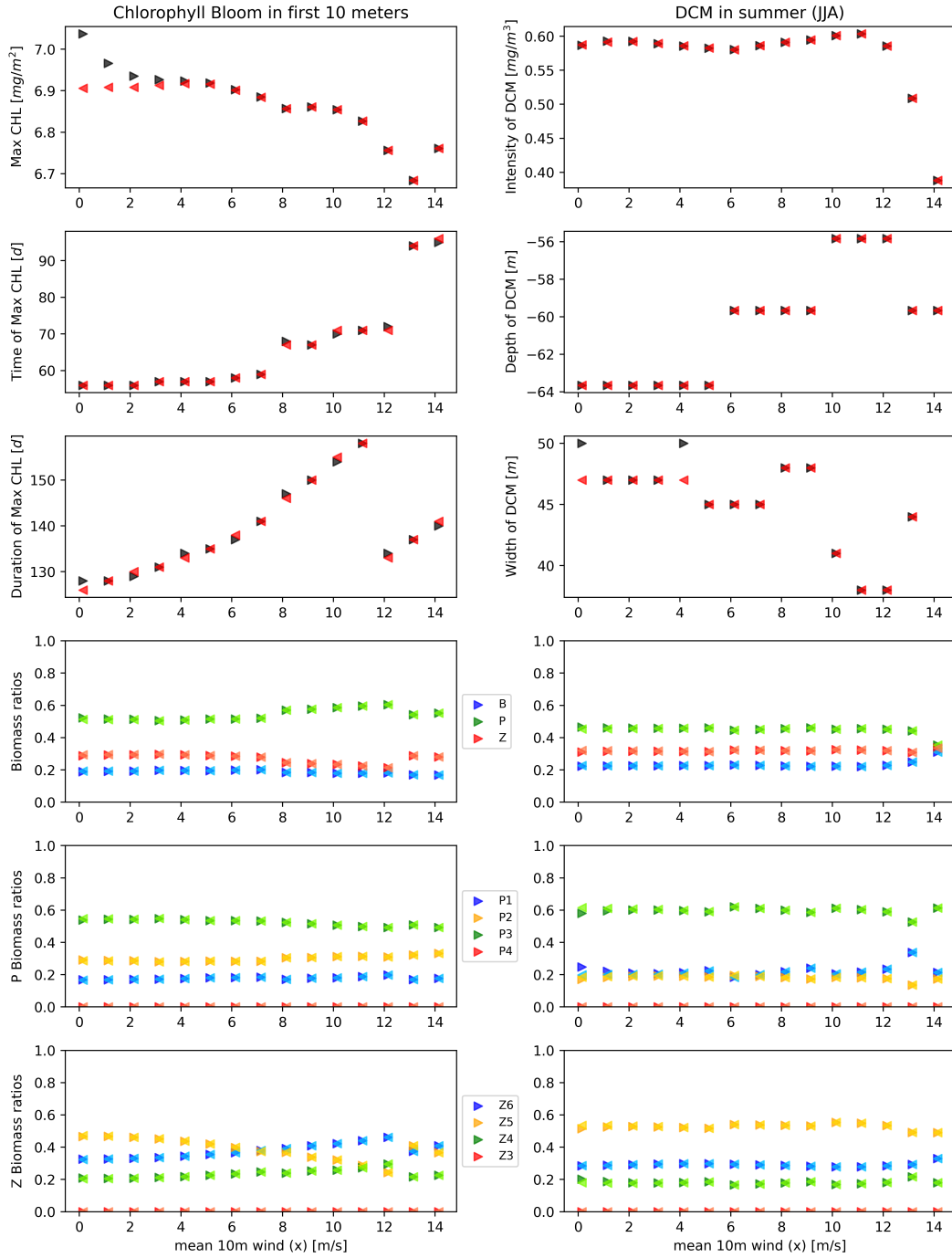
Fig. S1. Bifurcation diagrams for the dynamic regimes associated to Chlorophyll bloom (left panels) and DCM (right panels) under the variation of the wind forcing in the EXP-SEQ experimental setup. For each column, in the first three panels from the top the black triangles stand for the simulations which follow the x-axis values with time (forward), the red triangle the simulations which go backwards. For each column, in the first three panels from the bottom the darker coloured triangles stand for the simulations which follow the x-axis values with time, the lighted coloured triangles the simulations which go backwards, e.g. blue goes forward and light blue goes backward.
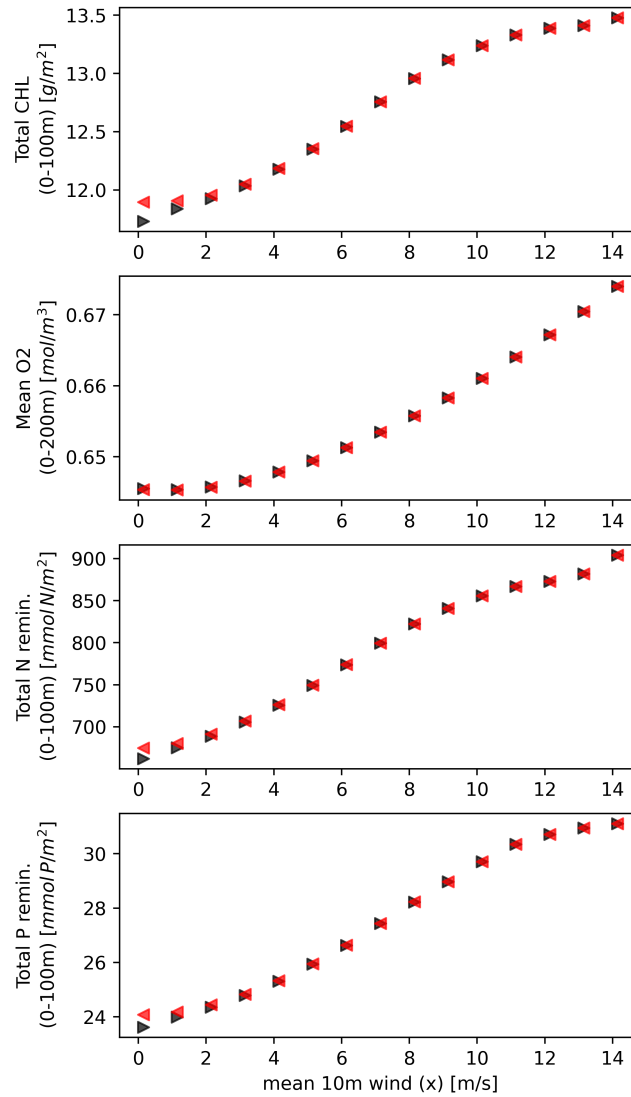
Fig. S2. Bifurcation diagrams under the variation of wind forcing in the EXP-SEQ experimental setup for the dynamic regimes associate with annual production and recycling: total chlorophyll produced each year in the first 100m, the total dissolved oxygen present in the first 200m produced each year, the total ammonium (N) remineralized in the first 100m each year and the total phosphate (P) remineralized in the first 100m each year. The black triangles stand for the simulation which follows the x-axis values with time, the red triangles the simulation which goes backwards.

Guido Occhipinti, Davide Valenti and Paolo Lazzari
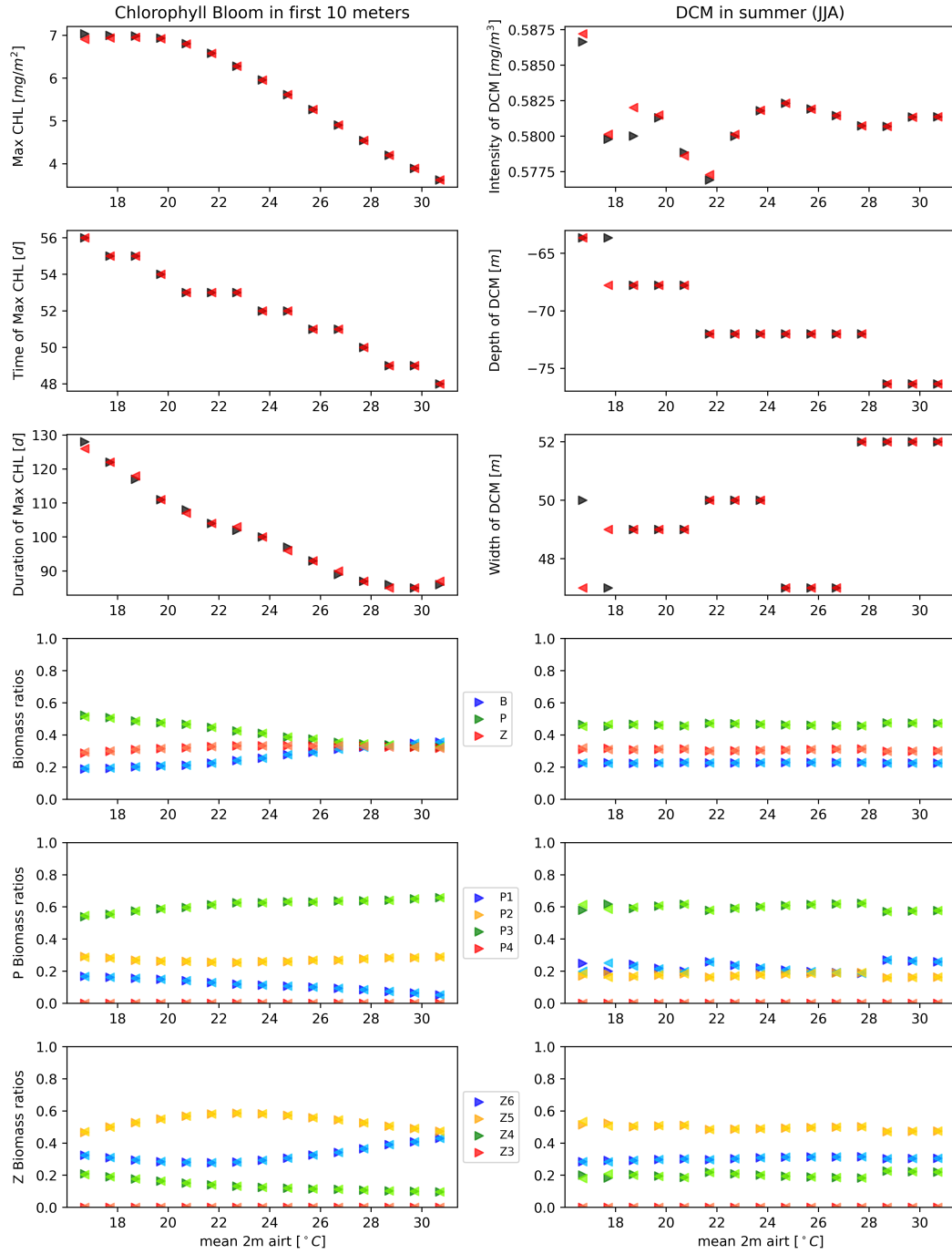
Fig. S3. Bifurcation diagrams for the dynamic regimes associated to Chlorophyll bloom (left panels) and DCM (right panels) under the variation of the air temperature forcing in the EXP-SEQ experimental setup. For each column, in the first three panels from the top the black triangles stand for the simulations which follow the x-axis values with time (forward), the red triangle the simulations which go backwards. For each column, in the first three panels from the bottom the darker coloured triangles stand for the simulations which follow the x-axis values with time, the lighted coloured triangles the simulations which go backwards, e.g. blue goes forward and light blue goes backward.
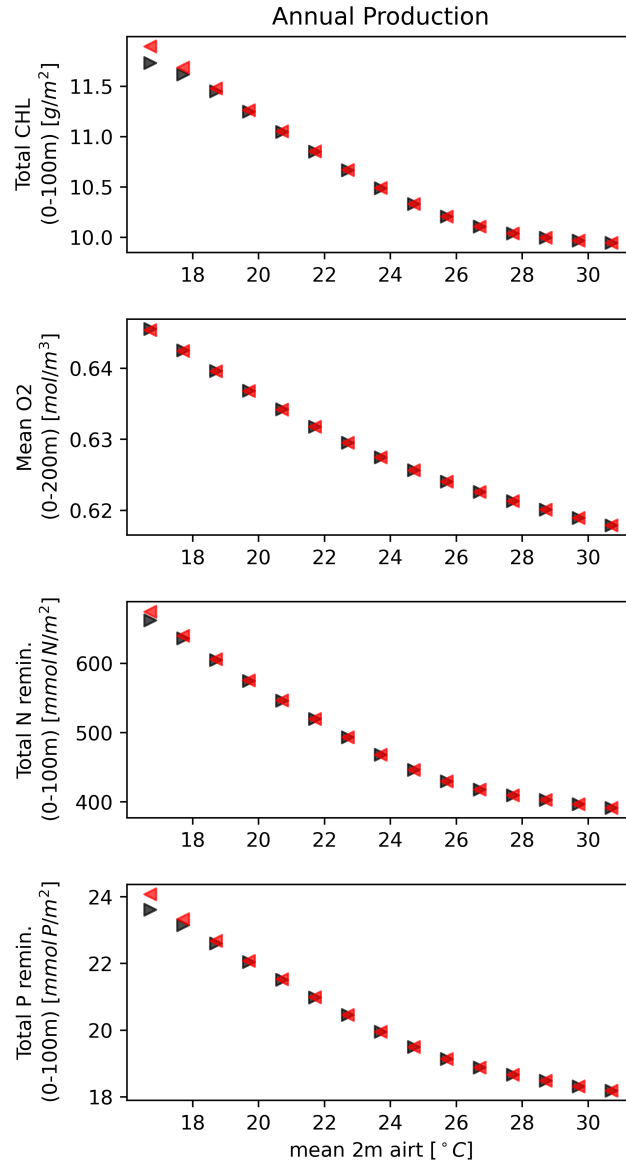
Fig. S4. Bifurcation diagrams under the variation of air temperature forcing in the EXP-SEQ experimental setup for the dynamic regimes associate with annual production and recycling: total chlorophyll produced each year in the first 100m, the total dissolved oxygen present in the first 200m produced each year, the total ammonium (N) remineralized in the first 100m each year and the total phosphate (P) remineralized in the first 100m each year. The black triangles stand for the simulation which follows the x-axis values with time, the red triangles the simulation which goes backwards.

Guido Occhipinti, Davide Valenti and Paolo Lazzari
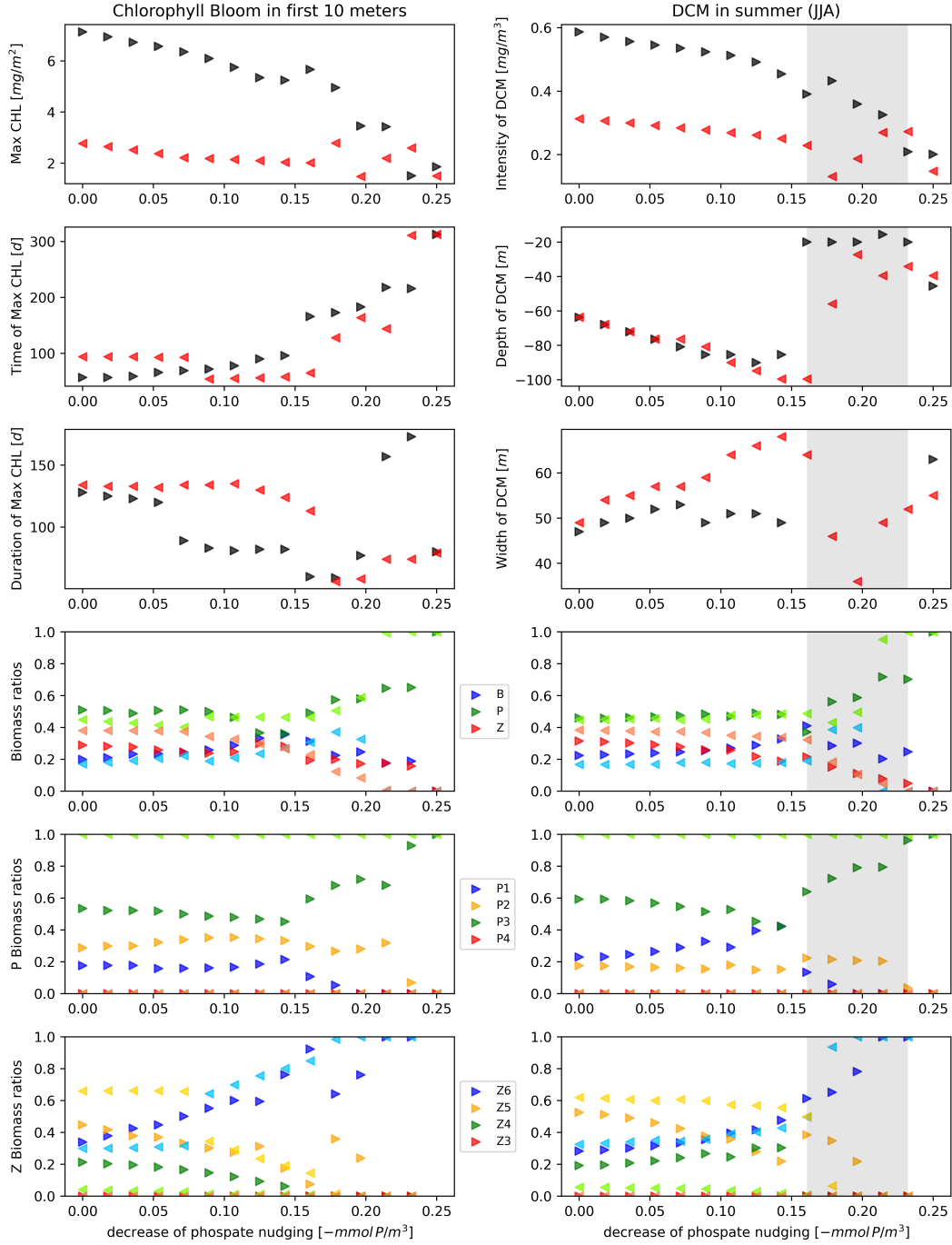
Fig. S5. Bifurcation diagrams for the dynamic regimes associated to Chlorophyll bloom (left panels) and DCM (right panels) under the variation of the phosphate nudging forcing in the EXP-SEQ experimental setup. For each column, in the first three panels from the top the black triangles stand for the simulations which follow the x-axis values with time (forward), the red triangle the simulations which go backwards. For each column, in the first three panels from the bottom the darker coloured triangles stand for the simulations which follow the x-axis values with time, the lighted coloured triangles the simulations which go backwards, e.g. blue goes forward and light blue goes backward. In the right panels the shaded region corresponds to the values of the 'Width of DCM' which identifies when the DCM does not exist anymore, i.e. DCM loses its structure and the chlorophyll is spread along the water column. The grey shade highlight the absence of the DCM only in the forward simulations.
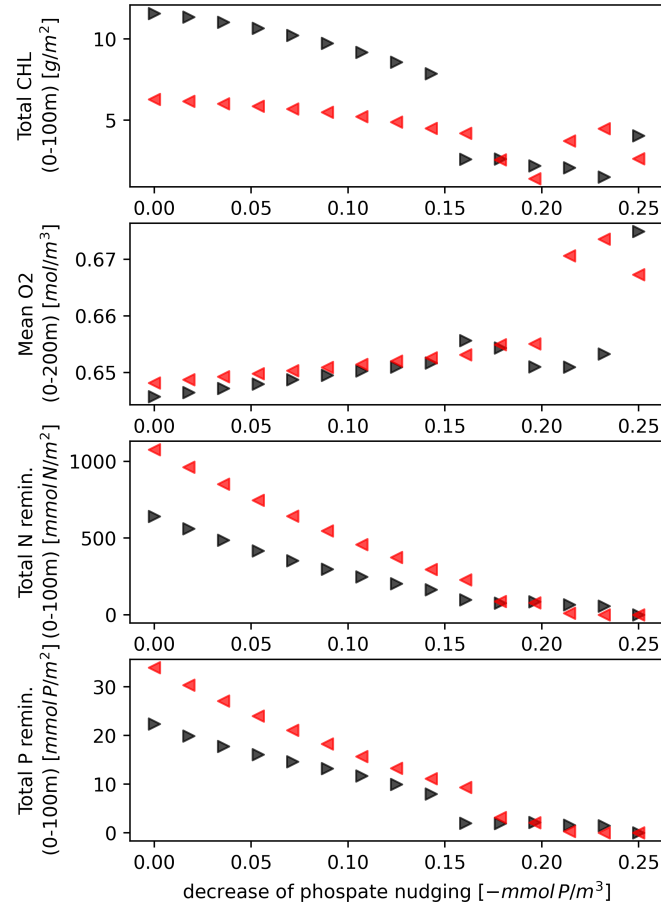
Fig. S6. Bifurcation diagrams under the variation of phosphate nudging forcing in the EXP-SEQ experimental setup for the dynamic regimes associate with annual production and recycling: total chlorophyll produced each year in the first 100m, the total dissolved oxygen present in the first 200m produced each year, the total ammonium (N) remineralized in the first 100m each year and the total phosphate (P) remineralized in the first 100m each year. The black triangles stand for the simulation which follows the x-axis values with time, the red triangles the simulation which goes backwards.

Guido Occhipinti, Davide Valenti and Paolo Lazzari
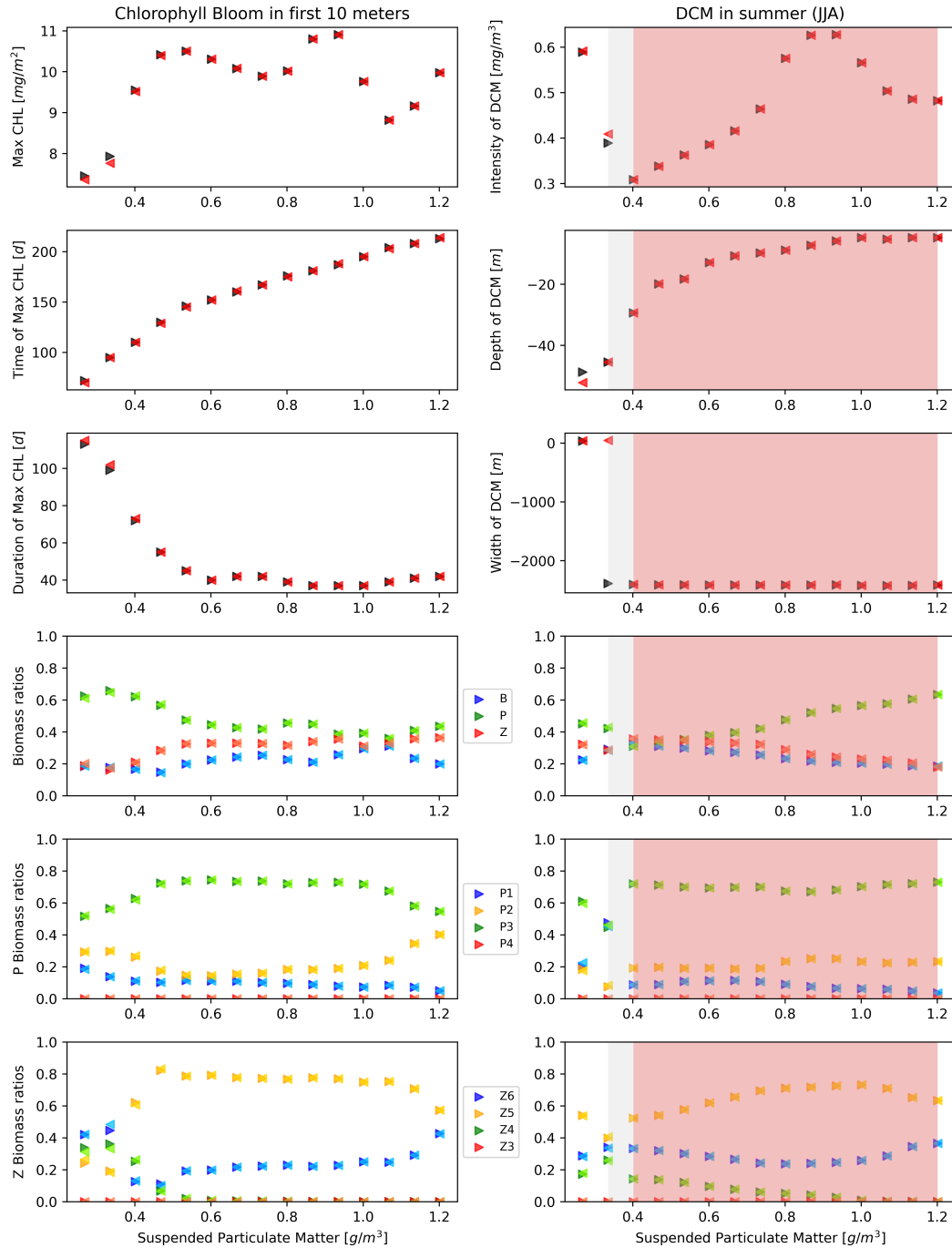
Fig. S7. Bifurcation diagrams for the dynamic regimes associated to Chlorophyll bloom (left panels) and DCM (right panels) under the variation of the suspended particulate matter (SPM) forcing in the EXP-SEQ experimental setup. For each column, in the first three panels from the top the black triangles stand for the simulations which follow the x-axis values with time (forward), the red triangle the simulations which go backwards. For each column, in the first three panels from the bottom the darker coloured triangles stand for the simulations which follow the x-axis values with time, the lighted coloured triangles the simulations which go backwards, e.g. blue goes forward and light blue goes backward. In the right panels the shaded region corresponds to the values of the 'Width of DCM' which identifies when the DCM does not exist anymore, i.e. DCM loses its structure and the chlorophyll is spread along the water column. A grey shade and a red shade are superimposed highlighting the absence of the DCM in both the forward and backward simulations.
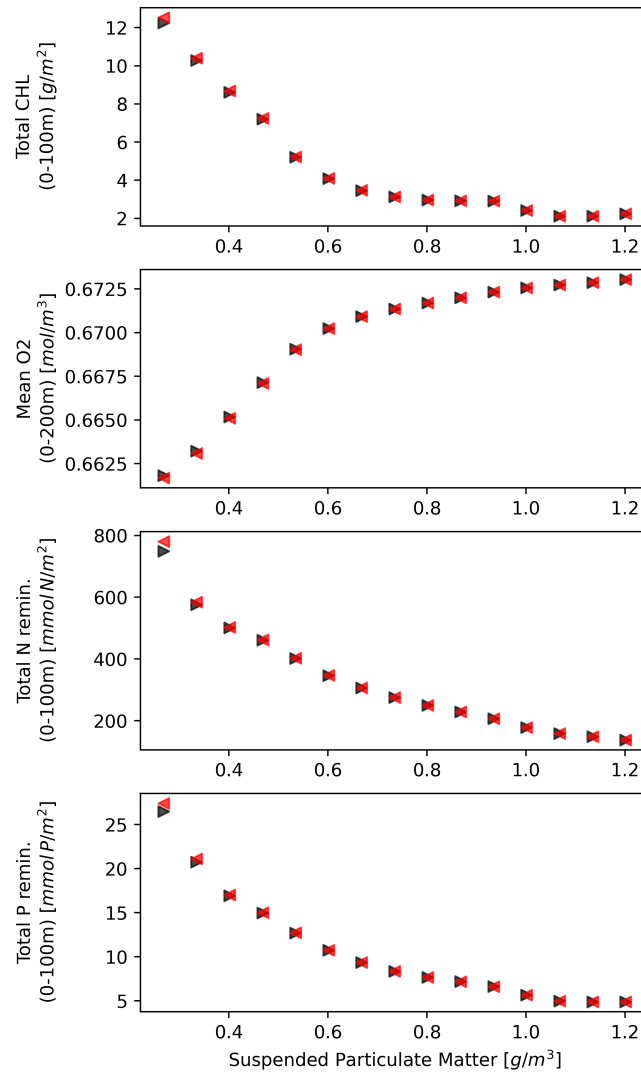
Fig. S8. Bifurcation diagrams under the variation of suspended particulate matter (SPM) forcing in the EXP-SEQ experimental setup for the dynamic regimes associate with annual production and recycling: total chlorophyll produced each year in the first 100m, the total dissolved oxygen present in the first 200m produced each year, the total ammonium (N) remineralized in the first 100m each year and the total phosphate (P) remineralized in the first 100m each year. The black triangles stand for the simulation which follows the x-axis values with time, the red triangles the simulation which goes backwards.
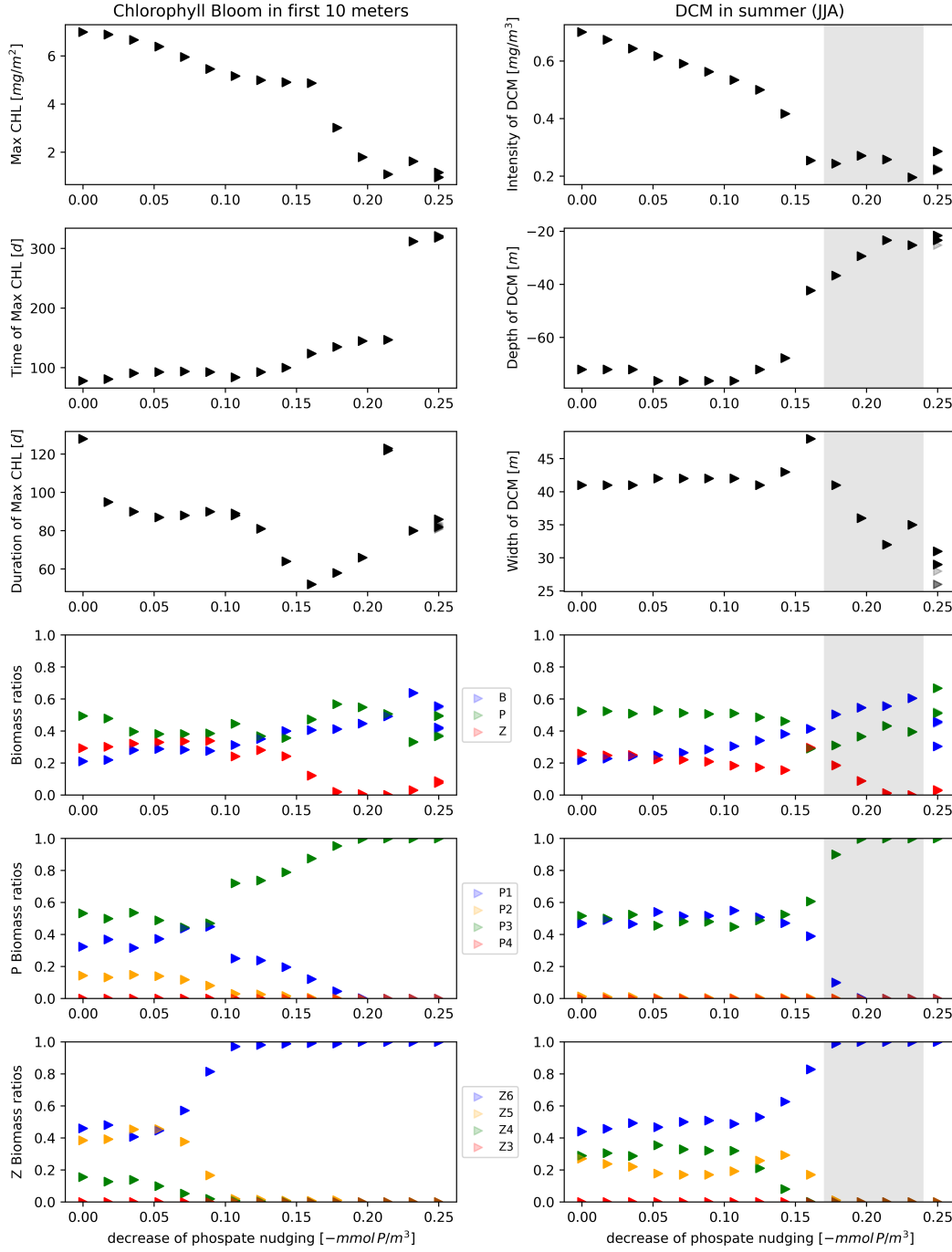
Fig. S9. Bifurcation diagrams for the properties of Chlorophyll bloom (left panels) and DCM (right panels) under the decrease of phosphate nudging. In the right panels the shaded region corresponds to the values of the 'Width of DCM' which identifies when the DCM does not exist anymore, i.e. DCM loses its structure and the chlorophyll is spread along the water column. For each value of the forcing (x-axis) 50 numerical solutions with different initial conditions are plotted. Multiple triangle for a single x-coordinate evidence the presence of multiple equilibria.
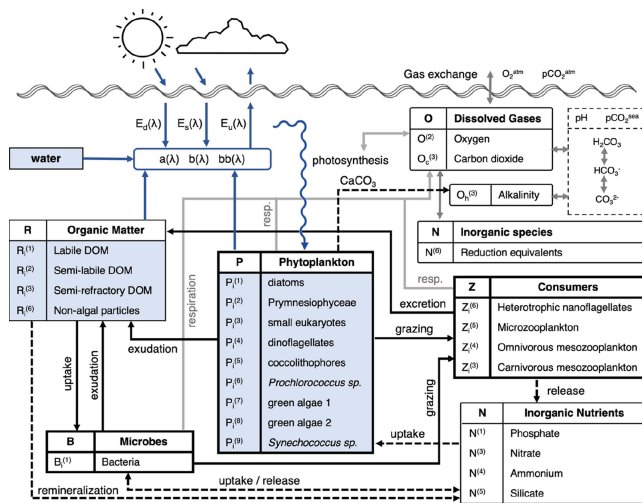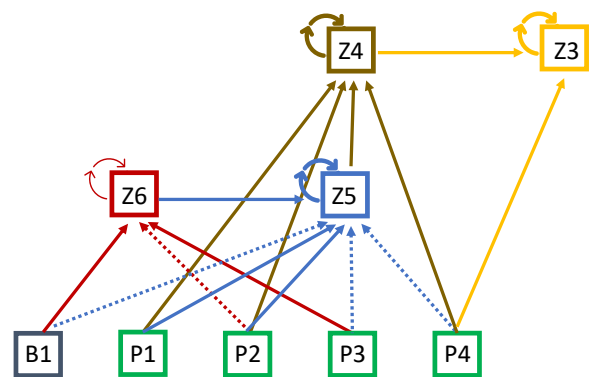
Fig. S10. (A) Scheme of the biogeochemical interactions between organisms within the BFM model. In blue the bio-optical interactions between biogeochemical variables and light. (B) Scheme of trophic web of BFM model. An arrow directed from one box to another indicates a predation flux. Solid arrows denote a higher preference for a specific prey, while dashed ones indicate a lower preference. A looping arrow on the box denotes cannibalism.
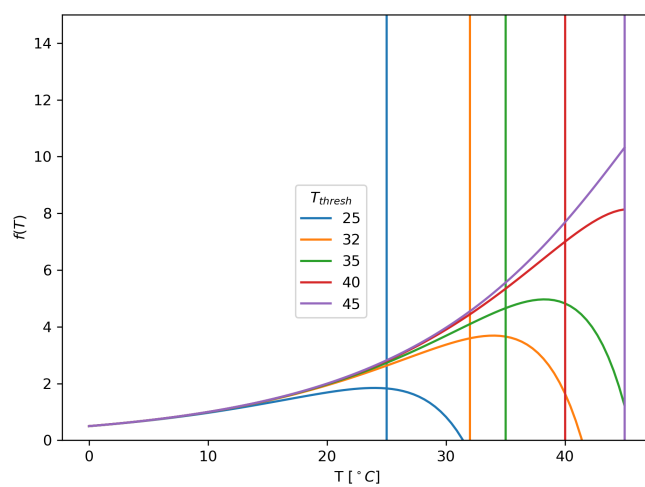
Fig. S11. Plot of the regulation function of temperature on metabolic rates (Eq. (4)). The value of the threshold temperature T_{thresh} set the flex of the function.

The first term represents phytoplankton uptake and $\sum_{j\in phytoP}$ runs over the phosphate components of the various phytoplankton functional types. The second term for bacterial uptake and release and $\sum_{j\in bacP}$ runs over the phosphate components of the different bacterial functional types, which is only one in the BFM. The last term for the excretion by zooplankton and $\sum_{j\in zooP}$ runs over the phosphate components of the various zooplankton functional types. The processes that take place in the nitrate cycle and are modelled in the BFM are the phytoplankton uptake, and the nitrification and denitrification processes. For ammonium, the BFM describes its consumption by the phytoplankton, the remineralization driven by bacteria and the excretion of urea by zooplankton, which is assumed to be directly available in the form of ammonium. The silicate cycle is modelled by diatom uptake and bacteria dissolution of silicate frustules.

Inorganic carbon is present in the ocean in three different forms: free carbon dioxide ($[CO_2] = [CO_2]_{aq} + [H_2CO_3]$), bicarbonate ions ($HCO_3^-$) and carbonate ions ($CO_3^{2-}$). These types of carbonate species reach equilibrium thanks to the following reactions:

$$CO_2 + H_2O \rightleftharpoons HCO_3^- + H^+ \rightleftharpoons CO_3^{2-} + 2H^+ \tag{10}$$

In the BFM, the seawater carbonate system is described by 7 chemical species, i.e, free carbon dioxide (CO_2), bicarbonate ions (HCO_3^-), carbonate ions (CO_3^{2-}), partial pressure of carbon dioxide in seawater (pCO_2), hydrogen ion concentration ($pH = -\log_{10}([H^+])$), dissolved inorganic carbon concentration (DIC) and total alkalinity (TA). $pCO2$ is needed to parameterize the gas exchange between air and ocean, while pH is of great interest given concerns about the ongoing acidification of the oceans.

Here we have described only some of the processes that are modelled by the BFM. There are many other state variables, such as different forms of dissolved organic matter (DOM), detritus and dissolved gases, e.g. oxygen. The complete list of equations and processes included in the BFM can be found in (7) and the BFM code manual in (8).

References

1. KJ Flynn, A mechanistic model for describing dynamic multi-nutrient, light, temperature interactions in phytoplankton. *J. Plankton Res.* **23**, 977–997 (2001).

2. JA Freund, S Mieruch, B Scholze, K Wiltshire, U Feudel, Bloom dynamics in a seasonally forced phytoplankton–zooplankton model: Trigger mechanisms and timing effects. *Ecol. Complex.* **3**, 129–139 (2006).

3. M Vichi, S Masina, Skill assessment of the pelagos global ocean biogeochemistry model over the period 1980–2000. *Biogeosciences* **6**, 2333–2353 (2009).

4. JA Raven, RJ Geider, Temperature and algal growth. *New Phytol.* **110**, 441–461 (1988).

5. JC Blackford, JI Allen, FJ Gilbert, Ecosystem dynamics at six contrasting sites: a generic modelling study. *J. Mar. Syst.* **52**, 191–215 (2004).

6. W Gentleman, A Leising, B Frost, S Strom, J Murray, Functional responses for zooplankton feeding on multiple resources: a review of assumptions and biological dynamics. *Deep. Sea Res. Part II: Top. Stud. Oceanogr.* **50**, 2847–2875 (2003).

7. P Lazzari, et al., Seasonal and inter-annual variability of plankton chlorophyll and primary production in the Mediterranean Sea: a modelling approach. *Biogeosciences* **9**, 217–233 (2012).

8. V M., et al., *The Biogeochemical Flux Model (BFM): Equation Description and User Manual*, (2020).